Reliable and Global Measurement of Fluorescence Resonance Energy Transfer Using Fluorescence Microscopes

Zongping Xia and Yuechueng Liu
Department of Pathology, University of Oklahoma Health Sciences Center, Oklahoma City, Oklahoma 73190 USA

ABSTRACT Green fluorescence protein (GFP)-based fluorescence resonance energy transfer (FRET) is increasingly used in investigation of inter- and intramolecular interactions in living cells. In this report, we present a modified method for FRET quantification in cultured cells using conventional fluorescence microscopy. To reliably measure FRET, three positive control constructs in which a cyan fluorescence protein and a yellow fluorescence protein were linked by peptides of 15, 24, or 37 amino acid residues were prepared. FRET was detected using a spectrofluorometer, a laser scanning confocal microscope, and an inverted fluorescence microscope. Three calculation methods for FRET quantification using fluorescence microscopes were compared. By normalization against expression levels of GFP fusion proteins, the modified method gave consistent FRET values that could be compared among different cells with varying protein expression levels. Whole-cell global analysis using this method allowed FRET measurement with high spatial resolutions. Using such a procedure, the interaction of synaptic proteins syntaxin and the synaptosomal associated protein of 25 kDa (SNAP-25) was examined in PC12 cells, which showed strong FRET on plasma membranes. These results demonstrate the effectiveness of the modified method for FRET measurement in live cell systems.

INTRODUCTION

Fluorescence resonance energy transfer (FRET) is a process of energy transfer from a fluorescent donor molecule to a fluorescent acceptor without the involvement of a photon (Förster, 1948; Stryer, 1978; Van der Meer et al., 1994). One result is that the fluorescence emission of the acceptor is enhanced by the excitation of the donor molecule, accompanied by a reduction in the donor emission. The efficiency of energy transfer is dependent on the molecular distance at an inverse sixth power. Therefore, FRET can be used as a highly specific molecular ruler (Stryer, 1978), and the technique has been used to study macromolecular interactions in both in vitro and in vivo systems. Many fluorophore pairs with proper spectra properties can be used for FRET experiments (Wu and Brand, 1994; Uster and Pagano, 1986; Jovin and Arndt-Jovin, 1989; Chapman et al., 1992; Clegg, 1996; Mason, 1999). More recently, the green fluorescent protein (GFP) from jellyfish *Aequorea victoria* was cloned (Chalfie et al., 1994), and several GFP variants including blue fluorescent protein (BFP), cyan fluorescent protein (CFP), GFP, and yellow fluorescent protein (YFP) have since been engineered (Heim and Tsien, 1996). The critical Förster radius is 40 Å for BFP-GFP and ~50 Å for CFP-YFP, suggesting that any significant FRET would indicate actual physical interaction between the two proteins. Because many proteins fused with GFP retain their physiological functions and subcellular targeting, FRET using GFP fusion proteins is becoming an increasingly popular and powerful tool for investigating protein-protein interactions in vivo (reviewed by Tsien, 1998; Pollok and Heim, 1999). For instances, CFP/YFP or BFP/GFP fusion protein pairs have been used to monitor calcium fluctuation in living cells (Miyawaki et al., 1997), bcl-2-bax interaction (Mahajan et al., 1998), synaptic activity in the synaptic spine (Vanderklish et al., 2000), and synaptic protein interactions (Xia et al., 2001).

Several methods using different instruments have been developed to measure FRET. These include spectrofluorometer (Olwin et al., 1982; Chapman et al., 1992), fluorescence lifetime imaging (Ng et al., 1999; Verveer et al., 2000), flow cytometry (Tron et al., 1984), laser scanning confocal microscopy (Wu and Brand, 1994), and conventional fluorescence microscopy (Youvan et al., 1997; Gordon et al., 1998). Conventional fluorescence microscopy provides a relatively simple and easy-to-use tool for FRET detection and measurement. In addition, it has the advantage over the other methods in live cell experiments that require high temporal/spatial resolutions (Wu and Brand, 1994). With specifically manufactured filter cubes, FRET can be measured under minimum background interference. Several quantification methods using fluorescence microscopes have been developed in recent years (Youvan et al., 1997; Gordon et al., 1998). In the present study, we use several FRET positive and negative controls to quantitatively measure FRET in living cells, and we describe here a modified FRET quantification method with improved reliability for global cell analysis.

Received for publication 8 March 2001 and in final form 9 July 2001.

Address reprint requests to Dr. Y. Liu, Department of Pathology, University of Oklahoma Health Sciences Center, P.O. Box 26901, Oklahoma City, OK 73190. Tel.: 405-271-2336; Fax: 405-271-3042; E-mail: yuechueng-liu@ouhsc.edu.

0006-3495/01/10/2395/08 $2.00

MATERIALS AND METHODS

Construction of CFP and YFP fusion proteins

A mouse cDNA encoding the synaptosomal associated protein of 25 kDa (SNAP-25*b*) was a generous gift from Dr. Michael C. Wilson (Scripps

Research Institute, San Diego, CA). cDNA encoding rat syntaxin 1A was a generous gift from Dr. Richard Scheller (Howard Hughes Medical Institute, Stanford, CA). pEYFP-N1, pECFP-N1, pECFP-C1, and pEYFP-C1 were from Clontech (Palo Alto, CA). An *Eco*RI site was introduced into the syntaxin cDNA at its ATG start codon and the *Eco*RI-*Apa*I fragment encoding syntaxin was ligated into the corresponding sites in pECFP-C1. YFP-SNAP-25 was constructed as previously described (Xia et al., 2001). For construction of CFP-YFP fusion proteins, CFP cDNA was cut out from pECFP-C1 and ligated to pEYFP-N1. Three constructs with different linker length between CFP and YFP were prepared: pCY-15 with 15 amino acid residues, pCY-24 with 24 residues, and pCY-37 with 37 residues.

Cell culture and transfection

PC12 cells were plated in 35-mm tissue culture dishes coated with 50 μg/ml poly-D-lysine, and the cells were cultured in Dulbecco's modified Eagle's medium (DMEM) supplemented with 10% fetal bovine serum (FBS) and 5% bovine calf serum. Nerve growth factor (GIBCO BRL, Gaithersburg, MD) was added to 50 ng/ml final concentration to induce differentiation. COS-7 cells were maintained in DMEM supplemented with 10% FBS in a humidified 37°C incubator with 5% CO_2. For transfection, the calcium phosphate method was used. Cells were split onto 35-mm tissue culture dishes at 70–80% confluency 1 day before transfection. Two micrograms of plasmid DNA were brought up to 45 μl with H_2O. In another tube, 5 μl of $CaCl_2$ of 2.5 M and 50 μl of buffer containing 50 mM BES (*N,N-bis*[2-hydroxyethyl]-2-aminoethanesultonic acid), 280 mM NaCl, 1.5 mM Na_2HPO_4, pH 6.95 were mixed. The two preparations were mixed and incubated at room temperature for 10 min. The DNA-calcium mixture was added drop-wise to cells. After mixing gently, the cells were maintained in an incubator at 37°C with 3.5% CO_2 for 24 h. On day 2, the media were replaced with fresh media, and the cells were incubated for 24 h before use.

Spectroscopic measurements of CFP-YFP fusion proteins in living cells

COS-7 cells were transfected with pCY-15, pCY-24, or pCY-37, as described above. After 48 h, the cells were collected and resuspended in PBS. The cell suspension was used directly for measurement using a spectrofluorometer (LS-50B, Perkin-Elmer, Norwalk, CT) without correction for the wavelength response of the system. The samples were measured in a quartz cuvette and excited at 425 nm (5-nm bandwidth), and emission spectra were collected from 450–550 nm (5-nm bandwidth). A sample co-transfected with pECFP-N1 and pEYFP-N1 was used as a negative control. The same amount of non-transfected COS-7 cells was used as a background control. The optical densities of the samples were 0.06–0.1. The final emission spectra were corrected for background, smoothed, and normalized.

Fluorescence microscopy, image acquisition, and preliminary FRET quantification

For detection of CFP, cells were viewed with an inverted fluorescence microscope (Leica DMIL with a 50-W X-Cite lamp from EFOS) under a filter set (all filters from Omega Optical, Mississauga, Ontario, Canada) with an excitation filter of 440/21 nm, a dichroic beam splitter of 455 nm, and an emission filter of 480/30 nm. YFP was viewed under a filter set with an excitation filter of 500/25 nm, a dichroic beam splitter of 525 nm, and an emission filter of 545/35 nm. The filters for FRET were 440/21 nm for excitation, 455 nm for dichroic beam splitter, and 535/26 nm for emission. Images were captured using a cooled CCD camera Quantix 57 (Photometrics, Tucson, AZ), a back-illuminated, frame-transfer camera utilizing a scientific grade EEV CCD57–10 chip. The camera was operated at 1 MHz with 12-bit digitization and controlled by IPlab 3.5 (Scanalytics, Fairfax, VA). The quantum efficiency for the back-illuminated CCD chip was ~80–83% in the 450–550-nm range, and the nonlinearity was ≤1%. Therefore, the variation in pixel response to CFP and YFP was considered minimum and insignificant.

Net FRET (*nF*) was calculated as follows (Youvan et al., 1997):

$$nF = I_{\mathrm{FRET}} - I_{\mathrm{YFP}} \times a - I_{\mathrm{CFP}} \times b, \tag{1}$$

Where I_{FRET}, I_{YFP}, and I_{CFP} are intensities in each region of interest (ROI) under FRET, YFP, and CFP filter sets, respectively. *a* is a norm of the percentage of CFP bleed-through, and *b* is a norm of the percentage of YFP bleed-through under the FRET filter set. There were no bleed-through signals from CFP under YFP filter sets and vice versa. The values for the bleed-through varied with different imaging systems. The norms *a* and *b* for the system used in the present study were 19% and 59%, respectively, which were determined by analyzing images of cells expressing only CFP or YFP and quantifying the relative intensity ratio under the FRET/CFP or FRET/YFP filter sets.

Normalization of FRET

It is evident that the *nF* calculated above can be affected by several factors: CFP and YFP intensity of the pixels and area of ROI selected, efficiency of FRET between CFP and YFP, and the complexes to free CFP and YFP ratio. So the *nF* should be normalized to make it comparable among ROIs within a cell and among different cells. An ideal mathematical normalization model for fluorescence microscopic FRET should meet two conditions: 1) it is a function of FRET efficiency between donor and acceptor and 2) it is a function of the ratio of complexes to total donor/acceptor:

$$\frac{[\mathrm{C_{d-a}}]}{[\mathrm{C_d}] + [C_{\mathrm{a}}]},$$

where $[\mathrm{C_{d-a}}]$ is the concentration of the donor-acceptor complexes, $[\mathrm{C_d}]$ is the total donor concentration, and $[\mathrm{C_a}]$ is the total acceptor concentration.

Theory

Set the following norms: *c*, YFP intensity per mole of YFP under YFP filter set; *d*, CFP intensity per mole of CFP under CFP filter set; *e*, CFP intensity per mole of CFP when having FRET with YFP under CFP filter set; *f*, net FRET intensity per mole of complex under FRET filter set; and *g*, molar ratio of YFP to CFP in a sample. Although it may vary between different samples, it should be a norm to a specific sample selected.

Norms *c* and *d* are determined by a particular fluorescence microscopy system (intensity of light source, filter sets, and sensitivity of image acquisition system) and are presumed to be constant with a specific system. Norms *e* and *f* are determined by FRET efficiency and are also constant for a specific FRET donor/acceptor pair, assuming minimum variations due to intermolecular orientation and conformational changes.

Set the following variables: *x*, [CFP] in moles; *y*, [CFP-YFP] complex in moles; *so*, [YFP] = *gx*; also, $y \le x$, and $y \le gx$.

Three normalization methods were defined and compared to determine which one(s) would meet those criteria as mentioned above.

$$\mathrm{FRETN} = \frac{nF}{I_{\mathrm{YFP}} \times I_{\mathrm{CFP}}} = \frac{fy}{cgx[ey + d(x - y)]} \tag{2}$$

$$N_{\mathrm{FRET}} = \frac{nF}{\sqrt{I_{\mathrm{YFP}} \times I_{\mathrm{CFP}}}} = \frac{fy}{\sqrt{cgx[ey + d(x - y)}} \tag{3}$$

$$nF/I_{\mathrm{CFP}} = \frac{fy}{ey + d(x - y)}, \tag{4}$$

where FRETN is the normalized value as described by Gordon et al. (1998), and N_{FRET} is the normalized FRET value described in the present study. Assuming that a complex is composed of a donor and an acceptor at a 1:1 ratio, the percentage of complex (P) exhibiting FRET to total donors and acceptors can be expressed as

$$P = \frac{2[\mathrm{CFP} - \mathrm{YFP}]}{[\mathrm{CFP}] + [\mathrm{YFP}]} = \frac{2y}{x + gx} = \frac{2y}{(1 + g)x}. \quad (5)$$

Resolving Eqs. 2–4 with Eq. 5 will result in

$$\mathrm{FRETN} = \frac{nF}{I_{\mathrm{YFP}} \times I_{\mathrm{CFP}}} = \frac{fy}{cgx[ey + d(x - y)]} = \frac{(1 + g)fP}{2cg[dx + (e - d)y]} \quad (6)$$

$$N_{\mathrm{FRET}} = \frac{nF}{\sqrt{I_{\mathrm{YFP}} \times I_{\mathrm{CFP}}}} = \frac{fy}{\sqrt{cgx[ey + d(x - y)]}} = \frac{(1 + g)fP}{\sqrt{2cg[2d + (1 + g)(e - d)P]}} \quad (7)$$

$$nF/I_{\mathrm{CFP}} = \frac{fy}{ey + d(x - y)} = \frac{(1 + g)fP}{2d + (1 + g)(e - d)P}. \quad (8)$$

Obviously, Eq. 6 does not meet the proposed criteria, in which FRETN is a function of FRET efficiency, complex percentage P, [CFP], and [CFP-YFP]. Equations 7 and 8 give normalized N_{FRET} and nF/I_{CFP} that are functions of FRET efficiency and complex percentage P. Equation 8, however, does not take into account YFP concentration. It is thus not suitable for comparison between two different samples.

For practical calculation purposes, there is no need to know the absolute values of norms c, d, e, and f, as knowing their relative values is enough to calculate the complex percentage P. Norms a and b can be readily determined as described above. Therefore, the measured I_{FRET}, I_{ECFP}, and I_{EYFP} can be used directly in Eqs. 9, 10, and 11.

Resolving the left parts of Eqs. 2–4 with Eq. 1 results in

$$\mathrm{FRETN} = \frac{I_{\mathrm{FRET}} - I_{\mathrm{YFP}} \times a - I_{\mathrm{CFP}} \times b}{I_{\mathrm{YFP}} \times I_{\mathrm{CFP}}} \quad (9)$$

$$N_{\mathrm{FRET}} = \frac{I_{\mathrm{FRET}} - I_{\mathrm{YFP}} \times a - I_{\mathrm{CFP}} \times b}{\sqrt{I_{\mathrm{YFP}} \times I_{\mathrm{CFP}}}} \quad (10)$$

$$nF/I_{\mathrm{CFP}} = \frac{I_{\mathrm{FRET}} - I_{\mathrm{YFP}} \times a - I_{\mathrm{CFP}} \times b}{I_{\mathrm{CFP}}}. \quad (11)$$

Global analysis of FRET in cells

A set of three images of a same field taken from CFP, YFP, and FRET filter sets were first subtracted for background and registered to ensure accurate pixel alignment in all images. The images were adjusted for threshold, changing the intensities of all pixels outside of the cell to zero. The new images were used to generate binary images with all values within the cell equal to 1 and outside equal to 0. Then the original images before threshold adjustment were multiplied by the binary image. This manipulation kept the pixel intensities unchanged within the cells, while leaving the pixel intensities to 0 outside of the cells. Bleed-through emission in the FRET images from direct excitation of CFP and YFP was subtracted using Eq. 1 to generate a net FRET (nF) image. Like the normalization methods for selected ROIs, the nF image was then normalized using Eq. 10 to generate a normalized FRET image. Image processing was performed using IPlab v3.5.

RESULTS

FRET from a CFP-YFP fusion protein

To reliably quantify FRET, a positive control fusion protein CY-15, in which CFP and YFP was linked by a 15-amino-acid peptide, was prepared. The fusion protein was expressed in COS-7 cells by transient transfection. As a negative control, COS-7 cells were co-transfected with CFP and YFP. FRET was detected using three different instruments: a fluorescence microscope, a laser scanning confocal microscope, and a spectrofluorometer. As shown in Fig. 1, although the spectrofluorometer measurement produced very reliable results, it had no spatial resolutions. The acceptor-photobleaching method using the laser scanning confocal microscope also generated accurate FRET results that showed an approximately twofold increase in CFP emission following YFP photobleaching. However, it was not suitable for live-cell studies due to the laser intensity. The conventional fluorescence microscopy method yielded similar results and demonstrated a strong FRET associated with the CY-15 fusion protein compared with the negative control samples (Fig. 1 *C*; Table 1) ($p < 0.01$).

Since epifluorescence microscopy is most suitable for live cell FRET studies, we compared three methods for detecting FRET using an epifluorescence microscope. A two filter system that uses FRET and donor filters provides a simple way to measure FRET (Adams et al., 1991; Wolf et al., 1992). As shown in Tables 1 and 2, the FRET-to-donor fluorescence ratio (nF/I_{CFP}) gave consistent FRET values with a standard error of <10%. However, nF/I_{CFP} is not normalized against donor and acceptor expression levels, which may vary significantly among different cells. Another procedure employs a three-filter system that calculates FRET value that is normalized against donor and acceptor levels (Gordon et al., 1998). It was effective detecting FRET-positive from FRET-negative samples (Table 2). This method, however, produced FRET values with large variations (standard error > 80%) that was affected by donor and acceptor concentrations (Table 2). It is suitable only for cells with well controlled donor/acceptor expression levels. Based on the three-filter system (Gordon et al., 1998), we have designed a formula (Eq. 10) that also normalizes against protein expression levels (see details in Materials and Methods). As shown in Tables 1 and 2, this method gave a more consistent FRET measurement with a standard error of <7%.

The three methods were used to perform direct pixel-by-pixel analysis in cells, which would visually show FRET intensities with high spatial resolution. Most image analysis

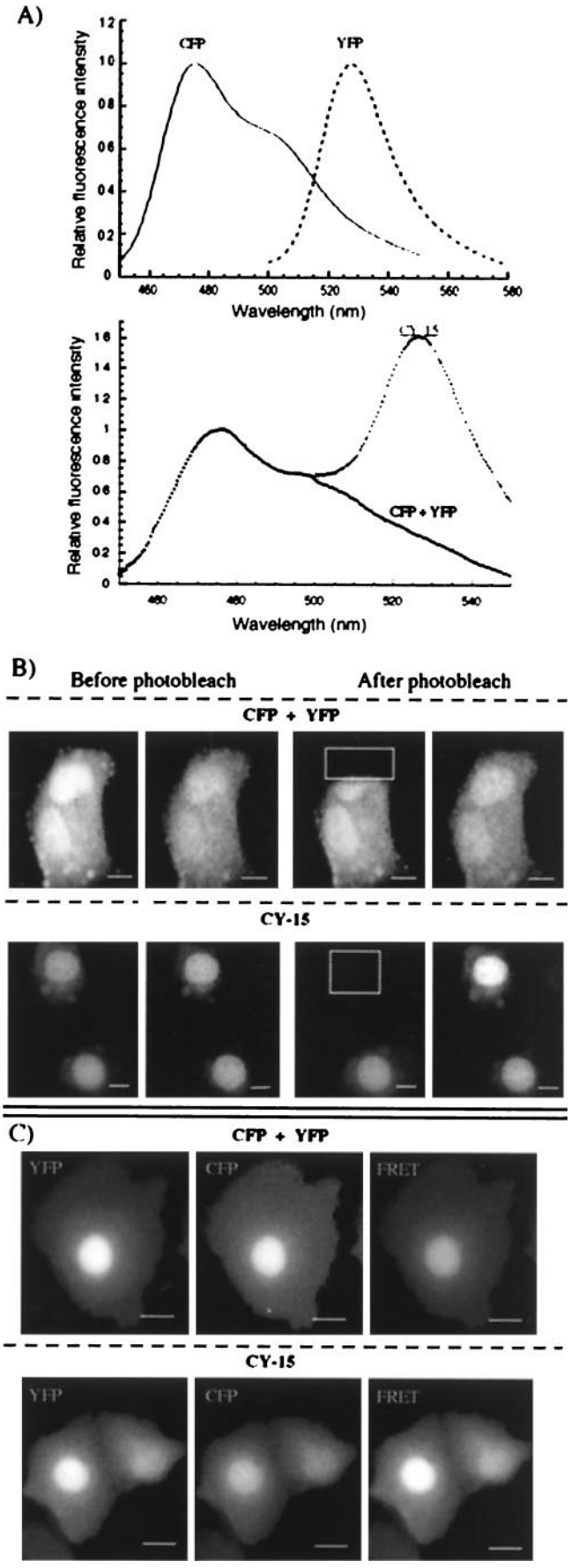

software allows image arithmetic and pixel-by-pixel adjustment. Using IPLab v3.5 from Scanlytics, we compared the three methods for FRET calculation. As illustrated in Fig. 2, both the modified method (N_{FRET}) and FRET-to-donor ratio (nF/I_{CFP}) gave relatively similar FRET values in the whole cells. The FRETN, however, had dramatically different values throughout the cells that were affected by protein concentrations.

To further demonstrate the effectiveness and reliability of the modified FRET calculation method, three additional CFP-YFP fusion proteins with different linker length were constructed. They were CY-24, which was linked by a 24-amino-acid sequence; CY-37, which was linked by a 37-amino-acid sequence; and Y-VA-C, which was linked by the synaptic vesicle associated protein VAMP-2 (Jacob et al., 2000). By spectrofluorometer measurement, CY-24 and CY-37 exhibited ~80% and 60% FRET efficiency compared with CY-15, respectively (Fig. 3). The Y-VA-C did not show any FRET using the same method (data not shown). The fusion proteins were expressed in COS-7 cells and examined using the fluorescence microscopy system. As shown in Table 1, all three calculation methods produced FRET values that were consistent with the spectrofluorometer measurement.

FRET measurement in cells with varying donor or acceptor levels

In experiments involving recombinant protein expression by gene transfection, it is often difficult to control precisely the protein expression levels in each cell. One of the requirements for FRET experiments is to reliably quantify FRET in cells independently of their protein expression levels. To test this, varying amounts of plasmids encoding CFP, YFP, or CY-15 were used in transfection experiments. Cells expressing various concentrations of CFP, YFP, or CY-15 were analyzed, and their CFP/YFP to CY-15 ratios were estimated by their measured fluorescence intensities (see Materials and Methods). As shown in Fig. 4, although the net FRET values did not reflect the number of interacting

FIGURE 1 Detection of FRET using three different instruments. COS-7 cells were transfected with CY-15 or co-transfected with CFP and YFP as described in Materials and Methods. (*A*) Emission spectrum properties of CFP and YFP alone when excited at 425 nm and 485 nm, respectively (*top panel*) and emission of CY-15 and control CFP + YFP when excited at 425 nm (*bottom panel*). Note that the emission of the acceptor YFP at 533 nm by CY-15 was increased, whereas no enhanced emission was detected with CFP + YFP. (*B*) The acceptor YFP was photobleached (the boxed area) using a laser scanning confocal microscope, leading to the increased emission of CFP; (*C*) By conventional fluorescence microscopy, the fluorescence intensity viewed under a FRET filter was significantly higher in cells expressing CY-15 compared with the negative control cells expressing CFP + YFP. Bar, 10 μm.

TABLE 1 Mean normalized FRET values for positive and negative controls

	FRETN*	N_{FRET}†	nF/I_{CFP}
CY-15	0.000832 ± 0.000669	0.796 ± 0.0495	1.323 ± 0.1296
CY-24	0.000561 ± 0.000100	0.740 ± 0.0196	1.163 ± 0.0393
CY-37	0.000523 ± 0.000074	0.689 ± 0.0277	1.098 ± 0.0670
Y-VA-C	0.00001 ± 0.00001	0.0376 ± 0.0471	0.0661 ± 0.0799
C + Y	0.0000063 ± 0.0000073	0.012 ± 0.0169	0.0157 ± 0.024

*Gordon et al., 1998.
†$N_{FRET} = nF/(I_{CFP} \times I_{YFP})^{1/2}$.

complexes in a cell, the N_{FRET} values were effective in distinguishing cells with differing complex concentrations.

Global analysis of protein-protein interactions in living cells

One advantage of GFP-based FRET is its ability to measure FRET in living cells and to study protein-protein interactions in its physiological environment (Tsien, 1998; Pollok and Heim, 1999). Using the formula (Eq. 10) and aided with an effective imaging system, it is possible to quantify FRET in cells with high spatial resolutions and to determine the subcellular locations where most interactions occur. For this purpose, the interaction of the neuronal SNARE proteins syntaxin and SNAP-25 was examined by FRET. Syntaxin and SNAP-25 are both presynaptic membrane proteins that participate in the formation of the SNARE core complex with synaptobrevin (also known as VAMP) during neuro-

TABLE 2 Quantification of FRET for CY-15 and CFP + YFP(C + Y)

	I_{FRET}*	I_{YFP}*	I_{CFP}*	FRETN†	N_{FRET}‡	nF/I_{CFP}
CY-15	7172	8288	2714	0.000178	0.843	1.472
	6005	7007	2284	0.000208	0.831	1.456
	5242	6060	2035	0.000234	0.823	1.420
	4290	5016	1643	0.000287	0.825	1.441
	3822	4214	1594	0.000310	0.803	1.305
	2871	3122	1212	0.000413	0.803	1.289
	2105	2333	944	0.000502	0.744	1.170
	1859	2172	845	0.000516	0.700	1.122
	1848	2089	834	0.000550	0.727	1.150
	1949	2057	855	0.000599	0.795	1.232
	1500	1577	710	0.000698	0.739	1.101
	1369	1543	525	0.000946	0.851	1.459
	1226	1403	494	0.000964	0.802	1.352
	1169	1297	445	0.001144	0.869	1.483
	1090	1220	436	0.001130	0.824	1.378
	983	1205	420	0.001000	0.712	1.205
	950	1053	395	0.001243	0.801	1.309
	537	606	222	0.002162	0.793	1.310
	471	542	178	0.002726	0.847	1.478
C + Y	4181	10517	3621	0.000001	0.008	0.013
	3841	9769	3360	0.000000	0.000	0.001
	2219	8769	922	0.000001	0.003	0.010
	2415	4113	2435	0.000020	0.062	0.081
	1139	3554	761	0.000005	0.009	0.019
	1061	2526	897	0.000023	0.034	0.058
	528	1406	439	0.000003	0.002	0.004
	528	1365	443	0.000012	0.009	0.016
	3392	1055	5390	0.000002	0.005	0.002
	3095	977	4865	0.000008	0.018	0.008
	2609	839	4138	0.000002	0.004	0.002
	2387	746	3792	0.000003	0.005	0.002
	2167	655	3463	0.000000	0.000	0.000
	1598	517	2525	0.000008	0.009	0.004

*Relative fluorescence intensity of ROIs after background subtraction.
†Gordon et al., 1998.
‡$N_{FRET} = nF/(I_{CFP} \times I_{YFP})^{1/2}$.

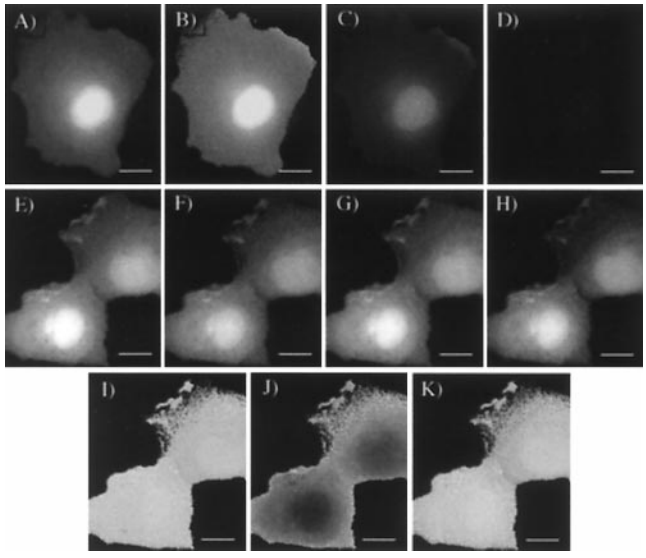

FIGURE 2 Global analysis of CY-15 in COS-7 cells using different methods. Images of cells expressing CY-15 were acquired as described in Materials and Methods. (*A–D*) Negative control cells expressing CFP + YFP; (*E–K*) FRET-positive cells expressing CY-15. Images were acquired under filters for YFP (*A* and *E*), CFP (*B* and *F*), and FRET (*C* and *G*). Net FRET (*D* and *H*) was calculated after pixel-by-pixel adjustment and image arithmetic as described in Materials and Methods. (*I*) Normalized FRET using Eq. 11; (*J*) normalized FRET using Eq. 9; (*K*) normalized FRET using Eq. 10. Bar, 10 μm.

secretion (reviewed by Südhof, 1995; Robinson and Martin, 1998). It is unclear from previous studies whether or not syntaxin and SNAP-25 exist as a binary complex in neurons during the resting state. To address this question, a CFP-syntaxin and YFP-SNAP-25 fusion protein were constructed and expressed in PC12 cells, which express endogenous SNAREs and have been used extensively for neurosecretion studies (Greene and Tischler, 1982; Martin and Kowalchyk, 1997). To achieve high spatial resolutions, we performed whole-cell FRET analysis following pixel-by-pixel adjustment and background subtraction. As shown in Fig. 5, syntaxin-SNAP-25 interaction was evident by the strong net FRET signals on plasma membranes. Because the N_{FRET} values are functions of both the FRET efficiency (distant dependent) and the ratio of complexed donor-acceptors to total donors and acceptors (concentration and affinity dependent), it would be difficult to determine which factor is the main cause in N_{FRET} changes using the fluorescence microscopy method. Nevertheless, if one could assume that protein complexes like syntaxin-SNAP-25 adopted a similar molecular conformation and orientation under steady-state conditions, the N_{FRET} values would reflect only the level of donor-acceptor complexes. As illustrated in Fig. 5 *E*, the N_{FRET} distribution was different from that of *nF*, suggesting that syntaxin-SNAP-25 complexes were differentially distributed along the plasma membranes.

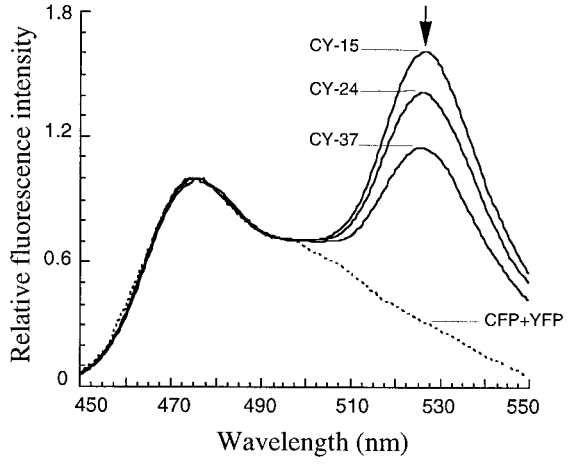

FIGURE 3 Emission spectra of CY-15, CY-24, and CY-37. COS-7 cells were transfected with CY-17, CY-24, or CY-37 as described in Materials and Methods. The cells were measured using a spectrofluorometer with the excitation at 425 nm. Note the increased FRET with the shorter linker peptides between CFP and YFP.

DISCUSSION

The main advantage of using GFP-based FRET is its ability to perform live-cell experiments. Coupled with an effective imaging system, GFP-based FRET technique can provide excellent temporal and spatial resolution that is not achieved with spectrofluorometer measurements. Although acceptor photobleaching using a laser scanning confocal microscope may provide a more accurate quantification of FRET, it is limited to experiments involving fixed cells. Similarly, any donor/acceptor-photobleaching FRET would not be suitable for monitoring dynamic FRET changes in vivo. It seems, therefore, that an epifluorescence microscope equipped with a digital camera provides the best solution for live-cell FRET studies, especially for those involving dynamic FRET changes caused by cell stimuli such as growth factors and ion fluctuations. Currently, only the relative FRET values were quantified and compared among samples under the same experimental conditions. Because FRET efficiencies can be accurately measured using the acceptor-photobleaching procedure, it should be possible in future studies to derive true energy transfer efficiencies with a combination of acceptor-photobleaching and fluorescence microscopy methods using the CFP-YFP fusion proteins described in this report.

A major concern for FRET measurement using fluorescence microscope is the so-called cross-talks between donor fluorescence and acceptor fluorescence and between FRET fluorescence and non-FRET fluorescence emitted from donor and/or acceptor (Gordon et al., 1998). In addition, FRET measurement is affected by a number of factors, e.g., quantum yield of fluorophores, photobleaching/quenching, and molecular position/orientation. Obviously, reliable positive and negative controls are essential for the accurate quanti-

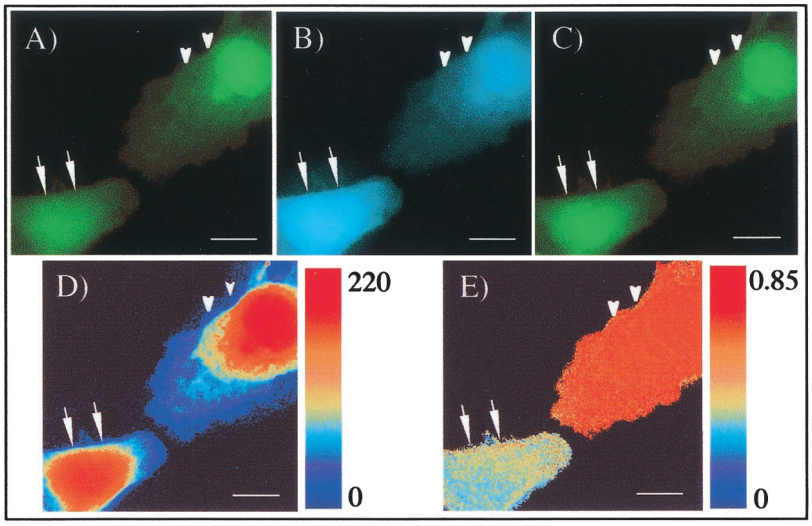

FIGURE 4 Normalized FRET values in cells expressing varying donor and acceptor levels. COS-7 cells were co-transfected with CY-15 and CFP. Cells with differential CY-15 expression were selected by their CYP to YFP molar ratio. The images were processed as described in Materials and Methods, and pseudo-colors were applied. (*A*) YFP fluorescence; (*B*) CFP fluorescence; (*C*) FRET fluorescence; (*D*) net FRET; (*E*) normalized FRET. Arrows indicate cells with 4:1 CFP to YFP ratio, and arrowheads indicate a cell with 2:1 CFP to YFP ratio. Note that the normalized FRETs were more evenly distributed in each cell and that the FRET value was a function of the percentage of CY-15 in the total recombinant proteins including both CY-15 and CFP. Color bars represent relative degree of net FRET and normalized FRET within the cells. Bar, 10 μm.

fication of FRET. A three-filter cube system such as the one used in the present study eliminates the cross-talk between donor and acceptor fluorescence with carefully selected fluorophore pairs. The photobleaching problem seemed to be minimum with GFP and its variants, because no significant loss of emission intensity following continuous illumination for 30 s with the 50-W arc lamp was observed (Xia and Liu, unpublished observation).

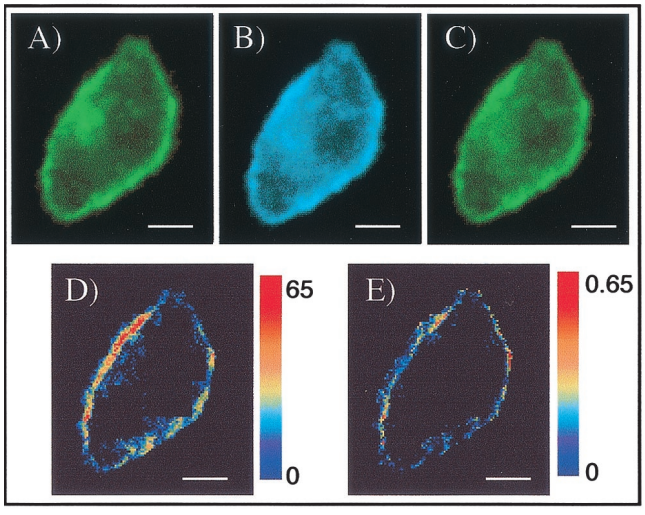

FIGURE 5 Global analysis of PC12 cell expression of CFP-syntaxin and YFP-SNAP-25. PC12 cells were transfected with CFP-syntaxin and YFP-SNAP-25 as described in Materials and Methods. Pseudo-color images were acquired under the three filter sets: YFP (*A*), CFP (*B*), and FRET (*C*). After subtraction of background and bleed-through signals, strong net FRET was localized to the plasma membranes (*D*). (*E*) Normalized FRET values using Eq. 10, showing strong FRET on the plasma membranes with a different pattern as compared with the net FRET in *D*. Color bars represent relative degree of net FRET and normalized FRET within the cells. Bar, 5 μm.

The two commonly used FRET values, I_{FRET}/I_{Donor} (or nF/I_{donor}) and FRETN, are effective detecting FRET signals as shown by previous reports and results in the present study (Gordon et al., 1998; Fig. 1 and Table 2). However, the former lacks comparability because it does not take into account the acceptor concentration. The FRETN values are limited to samples with comparable donor and acceptor concentrations. The method used in the present study is an attempt to provide a reliable FRET value that is also useful for comparison between different cells or samples. In experiments involving GFP fusion proteins, overexpression of the recombinant proteins may result in nonspecific interaction between the donor and acceptor. Purified GFP has been shown to dimerize at extremely high concentrations (>4 μM) in vitro (Heim, 1999). In our current system, however, no FRET was observed due to nonspecific interactions between the GFP molecules even in cases of overexpression (Fig. 1; Table 2). Another concern is the non-physiological interactions between recombinant proteins such as syntaxin and SNAP-25. Although this possibility cannot be entirely ruled out, several steps can be taken to minimize the probability of FRET from non-physiological interaction due to overexpression. One is to monitor functional changes as a result of recombinant protein expression. For instance, overexpression of syntaxin and SNAP-25 did not interfere with their normal function in neurosecretion (Zhou et al., 2000; Yang et al., 2000). Another approach is to perform global

FRET analysis as described in the current report. As shown in Fig. 5, both the net FRET (*nF*) and normalized FRET (N_{FRET}) values were distributed non-uniformly in the cell. Some areas such as the intracellular structures with high levels of syntaxin and SNAP-25 did not produce high FRET values (Fig. 5), suggesting that FRETs were more likely from physiological interactions of the two proteins. Finally, avoiding cells with high transgene expression should significantly reduce the probabilities for non-physiological interactions.

In addition to its usefulness as a molecular ruler, FRET can be used as a means to estimate the percentage of interacting molecules and the degree of complex formation. Assuming that the FRET efficiency is constant for each interacting pair, the FRET value is a function of the total number or the percentage of the interacting molecules. With a reliable calibration system, the ratio of complex to free molecules can be estimated using the method described in this report (Fig. 4). This approach is especially useful in whole-cell FRET analysis, where normalized FRET values illustrate the intensity and extent of molecular interactions. One must note, however, that it is difficult to achieve a perfect register for images acquired under the three-filter system. Artificial pixels may arise as a result of mis-registered images. This may be improved with specially fabricated filter cubes that produce precise spatial co-registration of all images (Youvan et al., 1997).

We thank Dr. Michael C. Wilson for the SNAP-25b clone and Dr. Richard Scheller for the syntaxin 1A cDNA clone. We also thank Dr. Mike Dresser for helping with confocal microscopy and Drs. Eric Howard, Jane Jacob, and Jialing Lin for helpful discussions and critical reading of the manuscript.

This work was supported by the National Institutes of Health (NS35167).

REFERENCES

Adams, S. R., A. T. Harootunian, Y. J. Buechler, S. S. Taylor, and R. Y. Tsien. 1991. Fluorescence ratio imaging of cyclic AMP in single cells. *Nature.* 349:694–697.

Chalfie, M., Y. Tu, G. Euskirchen, W. W. Ward, and D. C. Prasher. 1994. Green fluorescent protein as a marker for gene expression. *Science.* 263:802–805.

Chapman, E. R., K. Alexander, T. Vorherr, E. Carafoli, and D. R. Storm. 1992. Fluorescence energy transfer analysis of calmodulin-peptide complexes. *Biochemistry.* 31:12819–12825.

Clegg, R. M. 1996. Fluorescence resonance energy transfer. *In* Fluorescence Imaging Spectroscopy and Microscopy. X. F. Wang, and B. Herman, editors. Wiley, New York.179–252.

Förster, T. 1948. Intermolecular energy migration and fluorescence. *Ann. Phys. (Leipzig).* 2:55–75.

Gordon, G. W., G. Berry, X. H. Liang, B. Levine, and B. Herman. 1998. Quantitative fluorescence resonance energy transfer measurements using fluorescence microscopy. *Biophys. J.* 74:2702–2713.

Greene, L. A., and A. S. Tischler. 1982. PC12 pheochromocytoma cultures in neurobiological research. *Adv. Cell Neurobiol.* 3:373–414.

Heim, R. 1999. Green fluorescent protein forms for energy transfer. *Methods Enzymol.* 302:408–423.

Heim, R., and R. Y. Tsien. 1996. Engineering green fluorescent protein for improved brightness, longer wavelengths and fluorescence resonance energy transfer. *Curr. Biol.* 6:178–182.

Jacob, J. M., Q. Zhou, and Y. Liu. 2000. Novel method for the labeling of distant neuromuscular junction. *J. Neurosci. Res.* 61:61–66.

Jovin, T. M., and D. J. Arndt-Jovin. 1989. Luminescence digital imaging microscopy. *Annu. Rev. Biophys. Biophys. Chem.* 18:271–308.

Mahajan, N. P., K. Linder, G. Berry, G. W. Gordon, R. Heim, and B. Herman. 1998. Bcl-2 and Bax interactions in mitochondria probed with green fluorescent protein and fluorescence resonance energy transfer. *Nat. Biotechnol.* 16:547–52.

Martin, T. F., and J. A. Kowalchyk. 1997. Docked secretory vesicles undergo Ca^{2+}-activated exocytosis in a cell- free system. *J. Biol. Chem.* 272:14447–14453.

Mason, W. T. 1999. Fluorescent and Luminescent Probes for Biological Activity. Academic Press, New York.

Miyawaki, A., J. Llopis, R. Heim, J. M. McCaffery, J. A. Adams, M. Ikura, and R. Y. Tsien. 1997. Fluorescent indicators for Ca^{2+} based on green fluorescent proteins and calmodulin. *Nature.* 388:882–887.

Ng, T., A. Squire, G. Hansra, F. Bornancin, C. Prevostel, A. Hanby, W. Harris, D. Barnes, S. Schmidt, H. Mellor, P. I. H. Bastiaens, and P. J. Parker. 1999. Imaging protein kinase C activation in cells. *Science.* 283:2085–2089.

Olwin, B. B., C. H. Keller, and D. R. Storm. 1982. Interaction of a fluorescent *N*-dansylaziridine derivative of troponin I with calmodulin in the absence and presence of calcium. *Biochemistry.* 21:5669–5675.

Pollok, B. A., and R. Heim. 1999. Using GFP in FRET-based applications. *Trends Cell Biol.* 2:57–60.

Robinson, L. J., and T. F. Martin. 1998. Docking and fusion in neurosecretion. *Curr. Opin. Cell. Biol.* 10:483–492.

Stryer, L. 1978. Fluorescence energy transfer as a spectroscopic ruler. *Annu. Rev. Biochem.* 47:819–846.

Südhof, T. C. 1995. The synaptic vesicle cycle: a cascade of protein-protein interactions. *Nature.* 375:645–653.

Tron, L., J. Szollosi, S. Damjanovich, S. H. Helliwell, D. J. Arndt-Jovin, and T. M. Jovin. 1984. Flow cytometric measurement of fluorescence resonance energy transfer on cell surfaces: quantitative evaluation of the transfer efficiency on a cell-by-cell basis. *Biophys. J.* 45:939–946.

Tsien, R. Y. 1998. The green fluorescent protein. *Annu. Rev. Biochem.* 67:509–544.

Uster, P. S., and R. E. Pagano. 1986. Resonance energy transfer microscopy: observations of membrane-bound fluorescent probes in model membranes and in living cells. *J. Cell Biol.* 103:1221–1234.

Vanderklish, P. W., L. A. Krushel, B. H. Holst, J. Gally, K. L. Crossin, and G. M. Edelman. 2000. Marking synaptic activity in dendritic spines with a calpain substrate exhibiting fluorescence resonance energy transfer. *Proc. Natl. Acad. Sci. U.S.A.* 97:2253–2258.

Van der Meer, B. W., G. Coker, and S. Y. Chen. 1994. Resonance energy transfer: theory and data. VCH Publishers, New York.

Verveer, P. J., A. Squire, and P. I. H. Bastiaens. 2000. Global analysis of fluorescence lifetime imaging microscopy data. *Biophys. J.* 78: 2127–2137.

Wolf, D. E., A. P. Winiski, A. E. Ting, K. M. Bocian, and R. E. Pagano. 1992. Determination of the transbilayer distribution of fluorescent lipid analogues by nonradiative fluorescence resonance energy transfer. *Biochemistry.* 31:2865–2873.

Wu, P., and L. Brand. 1994. Resonance energy transfer: methods and applications. *Anal. Biochem.* 218:1–13.

Xia, Z., Q. Zhou, J. Lin, and Y. Liu. 2001. Stable SNARE complex prior to evoked synaptic vesicle fusion revealed by fluorescence resonance energy transfer. *J. Biol. Chem.* 276:1766–1771.

Yang, Y., Z. Xia, and Y. Liu. 2000. SNAP-25 functional domains in SNARE core complex assembly and glutamate release of cerebellar granule cells. *J. Biol. Chem.* 275:29482–29487.

Youvan, D. C., C. M. Silva, E. J. Bylina, W. J. Coleman, M. R. Dilworth, and M. M. Yang. 1997. Calibration of fluorescence resonance energy transfer in microscopy using genetically engineered GFP derivatives on nickel chelating beads. *Biotechnology.* 3:1–18.

Zhou, Q., J. Xiao, and Y. Liu. 2000. Participation of syntaxin 1A in membrane trafficking involving neutrite elongation and membrane expension. *J. Neurosci. Res.* 61:321-328.